Sundaralingam, M., Bergstrom, R., Strasburg, G., Rao, S. T., Raychowdhory, P., Greaser, M., & Wang, B. C. (1985) *Science 227*, 945–948.
Talbot, J. A., & Hodges, R. S. (1979) *J. Biol. Chem. 254*, 3720–3723.
Talbot, J. A., & Hodges, R. S. (1981) *J. Biol. Chem. 256*, 2798–2802.
Tsalkova, T. N., & Privalov, P. L. (1985) *J. Mol. Biol. 181*, 533–544.
Tsien, R. (1980) *Biochemistry 19*, 2396–2404.
Van Eyk, J. E., & Hodges, R. S. (1988) *J. Biol. Chem. 263*, 1726–1732.
Van Eyk, J. E., Cachia, P. J., Ingraham, R. H., & Hodges, R. S. (1986) *J. Protein Chem. 5*, 334–354.
Van Eyk, J. E., Kay, C. M., & Hodges, R. S. (1991) *Biochemistry 30*, 9974–9981.
Wang, C.-K., & Cheung, H. C. (1985) *Biophys. J. 48*, 727–739.
Wang, C.-L. A., Leavis, P. C., & Gergely, J. (1983) *J. Biol. Chem. 258*, 9175–9177.
Weber, G. (1975) *Adv. Protein Chem. 29*, 1–83.
Weeds, A. G., & Taylor, R. S. (1975) *Nature 257*, 54–56.
Weeks, R. A., & Perry, S. V. (1978) *Biochem. J. 173*, 449–457.
Wilkinson, J. M. (1974) *Biochim. Biophys. Acta 359*, 379–388.
Williams, D. L., Jr., & Swenson, C. A. (1982) *Eur. J. Biochem. 127*, 495–499.
Zot, H. G., & Potter, J. D. (1984) *Met. Ions Biol. Syst. 17*, 381–410.
Zot, A. S., & Potter, J. D. (1987) *Annu. Rev. Biophys. Biophys. Chem. 16*, 535–559.

# Role of Protein–Protein Interactions in the Regulation of Transcription by *trp* Repressor Investigated by Fluorescence Spectroscopy†

Teresa Fernando‡ and Catherine Royer*,§

*School of Pharmacy, University of Wisconsin—Madison, 425 North Charter, Madison, Wisconsin 53706, and Department of Biochemistry, University of Illinois, 1209 West California, Urbana, Illinois 61801*

*Received October 14, 1991; Revised Manuscript Received January 31, 1992*

ABSTRACT: In the present work, we have characterized the protein–protein interactions in the *trp* repressor (TR) from *Escherichia coli* using fluorescence spectroscopy. The steady-state and time-resolved fluorescence anisotropy of repressor labeled with 5-(dimethylamino)naphthalene-1-sulfonamide (DNS) was used to monitor subunit equilibria in the absence and presence of corepressor. In the absence of tryptophan, the repressor is in equilibrium between tetramers and dimers in the concentration range studied (approximately 0.04–40 μM in dimer). Binding of corepressor resulted in a marked destabilization of the tetramer. The beginning of a dimer–monomer dissociation transition was observed by monitoring the decrease in the intrinsic tryptophan emission energy upon dilution below 0.1 μM in dimer, indicating an upper limit for the dimer-dissociation constant near 1 nM. DNA titrations with a 26 base pair sequence containing the *trp* EDCBA operator performed in the absence and presence of the corepressor are consistent with a 1:1 dimer/operator stoichiometry in the presence of tryptophan, while the aporepressor binds with TR dimer/DNA stoichiometries greater than one and which depend upon both the concentration of protein and that of the operator. Using the multiple observable parameters available in fluorescence, we have thus carried out a thorough investigation of the coupled equilibria in this bacterial repressor. Our results are consistent with a physiologically relevant thermodynamic role for tetramerization in the regulatory function of the *trp* repressor. The present results which have brought to light novel protein–protein interactions in the *trp* repressor system indicate that fluorescence spectroscopic methods could prove quite useful in the study of the role of protein–protein interactions in eukaryotic systems as well.

Protein–protein interactions have emerged as one of the underlying general mechanisms governing the regulation of transcription. Such protein oligomerization interactions intervene in regulating the binding to DNA by prokaryotic repressors such as the *arc* (Bowie & Sauer, 1989), *lambda* (Senear & Ackers, 1990), and *lac* repressors (Royer et al., 1990). Differential dimerization affinities are involved in the activation of eukaryotic transcription by the oncogene products fos and jun (Turner & Tijan, 1989; Gentz et al., 1989; Kouzerides & Ziff, 1989), which also play a role through protein–protein interactions in modulating the activity of hormonal receptors (Diamond et al., 1990). Both positive and negative regulating dimerization partners have been identified for a number of helix–loop–helix-type proteins implicated in development and differentiation (Baringa, 1991; Blackwood & Eisenman, 1991; Prendergast et al., 1991). The three-dimensional structure for several DNA-binding proteins, both alone and complexed with their cognate DNA sequences, have been solved, including those of the *trp* repressor (Schevitz et al., 1985; Zhang et al., 1987; Otwinowski et al., 1988), and these provide the framework for an understanding of their function. However, a complete understanding of the physi-

† This work was supported by a grant to C.A.R. from the National Institutes of Health (R-29-GM39969).
* To whom correspondence should be addressed.
‡ University of Illinois.
§ University of Wisconsin—Madison.

0006-2960/92/0431-3429$03.00/0 

cochemical mechanisms of transcriptional control necessitates the characterization of the free energies involved in the multiple protein–ligand, protein–DNA, and protein–subunit equilibria, since these constitute the driving forces for regulatory events. It has become quite clear that it is particularly important not to neglect the study of protein–protein interactions in these systems, as they provide a crucial level of control by which changes in cellular concentrations of particular polypeptides can affect the levels of transcription by shifting the protein oligomerization equilibria. In the present work, we have used a number of fluorescence spectroscopic approaches to study the subunit interactions of the *trp* repressor (TR)[1] from *Escherichia coli* and how these may be energetically coupled to corepressor and DNA binding.

TR is involved in the regulation of transcription of the genes of the *trp* EDCBA, *aroH*, and *trpR* operons in response to changes in the concentration of tryptophan in the environment (Brown, 1968; Rose et al., 1973; Bennett et al., 1976; Gunsalus & Yanofsky, 1980). In regulating the expression of the *trp* EDCBA operon, TR binds specifically to an operator sequence within the *trp* EDCBA promoter region, competing with the RNA polymerase for binding, and thus effectively repressing transcription. This specific binding, which exhibits a dissociation constant of approximately 0.5 nM (Carey, 1988), requires the presence of the corepressor L-tryptophan (Rose et al., 1973; Rose & Yanofsky, 1974; Joachimiak et al., 1982; Klig et al., 1987; Carey, 1988). The dissociation constant for nonspecific interaction with DNA is near $10^{-7}$ M (Carey, 1988). As Carey pointed out in the discussion of her results, this means that the specificity ratio is only about 200, which is rather low to explain efficient repression in vivo. For comparison, the specificity ratio for the *lac* repressor is near $10^5$.

Two corepressor molecules bind per TR dimer, and each of these makes contacts with both subunits (Schevitz et al., 1985; Otwinowski et al., 1988). The structure of the dimer is also quite complex in that the interface between the monomeric subunits is formed by interlocking $\alpha$-helices from each subunit (Schevitz et al., 1985; Zhang et al., 1987). At low protein concentrations and in presence of tryptophan, conditions which correspond to the specific binding regime of the protein to its cognate DNA sequence, the bound TR is in a dimeric form (Carey, 1988; Otwinowski et al., 1988), and the bound corepressor contributes both direct and indirect contacts to the interaction with DNA (Otwinowski et al., 1988). Gel retardation assays, methylation protection experiments, and DNase footprinting patterns provide evidence that, at higher concentrations of repressor, more than one repressor dimer is bound to the DNA (Bass et al., 1987; Kumamoto et al., 1987; Carey, 1988; Staake et al., 1990). While this binding of multiple TR dimers only occurs at much higher protein concentrations than does the high-affinity binding, these concentrations (0.1–1 $\mu$M) are comparable to the in vivo cellular concentration of the repressor (Gunsalus et al., 1986). The DNA binding stoichiometries and the low specificity ratio led us to ask what the role of protein–protein interactions may be in determining the mode of TR binding to DNA.

In order to monitor the protein–protein and protein–DNA binding equilibria in this system, the steady-state and time-resolved fluorescence anisotropy of TR labeled with the long-lived fluorescence probe 5-(dimethylamino)-naphthalene-1-sulfonamide or DNS have been investigated as a function of protein concentration, tryptophan, and 26-mer operator concentration. The long lifetime of DNS, 10–15 ns, is well suited to the observation of the tumbling of macromolecules in solution. Another distinct advantage of labeling the repressor with the extrinsic DNS probe stems from the fact that the excitation of the DNS probe is centered near 350 nm, well beyond the absorption band of tryptophan, and its emission is centered at 500 nm, well beyond the emission spectrum of tryptophan. We were therefore able to examine the effects of corepressor binding upon the subunit equilibria in TR-DNS. The anisotropy of fluorescence ($A$) is calculated from the parallel and perpendicular fluorescence emission intensities as follows:

$$A = (I_{\parallel} - I_{\perp})/(I_{\parallel} + 2I_{\perp}) \quad (1)$$

If there is no motion of the fluorophore during the lifetime of the excited state, then the measured anisotropy ($A$) will be equal to the limiting anisotropy ($A_0$) of the fluorophore, which is determined by the angle between absorption and emission dipoles. However, if the fluorophore undergoes reorientation during its excited state lifetime, then one observes a decrease in the value of the anisotropy as compared to the limiting value. In the case of fluorophores covalently bound to macromolecules, the value of the observed steady-state anisotropy results from a combination of depolarization due to global macromolecular tumbling as well as local motions of the fluorophore. Dilution of a sample of oligomeric protein in the appropriate concentration range results in a shift of the subunit interaction equilibria toward the dissociated species due to mass action. Since the size of the dissociated form of the oligomer is smaller than its associated form, it will tumble faster in solution. This decrease in the correlation (or tumbling) time leads to an overall decrease in the measured fluorescence anisotropy. The anisotropy changes may also reflect differences in probe mobility in the different oligomeric states. Nonetheless, any protein concentration dependent anisotropy change is necessarily the result of a shift in protein subunit equilibria.

The observed steady-state anisotropy is also dependent upon the lifetime ($\tau$) of the fluorophore as well as its correlation time ($\tau_c$):

$$(A_0/A) - 1 = \tau/\tau_c \quad (2)$$

An increase in the fluorescence lifetime with no change in the correlation time, for example, would result in a steady-state anisotropy value which would be lower than if there had been no change in lifetime. However, we point out that a change in any fluorescence parameter (lifetime, color, normalized intensity) which is the consequence of a change in protein concentration is necessarily a result of a shift in the binding equilibria between the polypeptide chains. Therefore, lifetime

[1] Abbreviations: TR, *trp* repressor from *E. coli*. This does not refer to repressor ligated with L-tryptophan; DNS, 5-(dimethylamino)-naphthalene-1-sulfonamide. This is the protein-bound form; 26-mer, the 26 base pair oligonucleotide containing the *trp* EDCBA operator sequence.

5'-CATCGAACTAGTTAACTAGTACGCAA-3'

3'-GTAGCTTGATCAATTGATCATGCGTT-5'

bp, base pair; $A$, anisotropy of fluorescence emission. A subscripted t refers to time-resolved anisotropy; $A_0$, limiting anisotropy, determined by the angle between the absorption and emission dipoles. This is a constant for each fluorophore; $\tau$, fluorescence lifetime. A subscripted $i$ or number refers to a particular component in a complex decay; $\alpha_i$, preexponential weighting factor or relative concentration for lifetime component $i$; $f_i$, fractional contribution of component $i$ to the total fluorescence intensity; $\tau_c$, correlation time. This is the general symbol. When referring to an average value, this is indicated in the text; $\tau_w$, local fluorophore wobbling correlation time, also referred to in the text and Table II as $\tau_{c2}$; $\tau_{cp}$, correlation time arising from global tumbling of the macromolecule in solution, also referred to as $\tau_{c1}$ in Table II; $\theta_0$, half-angle for the cone in which the fluorophore is modeled to undergo local wobbling motions; $\eta$, solution viscosity; $V_h$, hydrated volume of the macromolecule in cm$^3$/mol.

changes can influence the shape of an anisotropy dilution profile but can by no means constitute its only origin.

In order to evaluate the relative contributions to the steady-state anisotropy of lifetime changes, as well as local motion versus global molecular tumbling, we have used time-resolved fluorescence techniques to further characterize the anisotropy dilution profile. Because the local rotational motions of the probe occur on a much faster time scale than the global macromolecular tumbling, they can be differentiated in a time-resolved experiment. Another method for differentiating between the local and global rotational motions of the DNS probe on a macromolecule is to vary the viscosity in a rather low viscosity range. As the viscosity ($\eta$) increases, the global tumbling of the macromolecule is slowed. The extent to which this effect is observed in steady-state anisotropy ($A$) measurements as a function of viscosity is related to the size of the macromolecule through the Perrin equation (Perrin, 1926; Weber, 1966):

$$1/A = 1/A_0(1 + [RT\tau/\eta V_h)] \quad (3)$$

where $A_0$ is the limiting anisotropy of the probe, $\tau$ is the average lifetime, and $V_h$ is the hydrated volume of the macromolecule. We have performed Perrin experiments as a function of TR and tryptophan concentration as a means of further characterizing the oligomerization properties of TR.

When TR binds to a DNA oligonucleotide, the macromolecular complex is larger in size than the TR alone. We have therefore used the anisotropy of the DNS-labeled TR in order to study its binding to a 26-mer containing the *trp* EDCBA operator sequence.

5'-CATCGAACTAGTTAACTAGTACGCAA-3'

3'-GTAGCTTGATCAATTGATCATGCGTT-5'

In addition to studies using the DNS-labeled repressor, we have investigated the subunit and operator binding equilibria in absence of corepressor using the intrinsic tryptophan emission of TR. The protein concentration dependence of the intrinsic anisotropy, as in the DNS experiments, reports on the subunit interactions. The anisotropy of the intrinsic fluorescence of TR as a function of operator 26-mer was employed as a means of monitoring the binding of the aporepressor to its cognate DNA sequence.

## Materials and Methods

*Protein Purification.* An *E. coli* strain, CY15071, which overproduces the *trp* repressor (Paluh & Yanofksy, 1986) was obtained from Dr. Kathleen Matthews, Rice University. TR was purified according to Paluh and Yanofsky (1986), Joachimiak et al. (1983), or He and Matthews (1989) with the following changes. Cells were suspended in 100 mL of 0.1 M Tris-HCl, pH 7.5, for each 60 g of cells. They were broken by three successive passages through a pressurized extruder. The extract was centrifuged for 20 min at 10000 rpm on a Sorvall RC-5B centrifuge with a GS3 rotor at 4 °C. Streptomycin sulfate was added while stirring to the supernatant to a final concentration of 1%. The solution was stirred at 4 °C for 60 min and then heated to 62 °C for 5 min. A large amount of precipitate formed at this step. The mixture was cooled on ice to 15 °C and then centrifuged for 20 min at 10000 rpm. The supernatant was precipitated with 45% ammonium sulfate, stirred in the cold room for 45 min, centrifuged for 20 min at 10000 rpm and reprecipitated with 75% ammonium sulfate. After being stirred in the cold for 60 min, the solution was centrifuged for 20 min at 10000 rpm. The pellet was then resuspended in 10 mM potassium phosphate, 0.1 M KCl, and 0.1 mM EDTA, pH 7.6. A 400-mL phosphocellulose column was equilibrated with 10 mM potassium phosphate, 0.2 M KCl, and 0.1 mM EDTA, pH 7.6, until the elution buffer had the same pH and conductivity as the starting buffer. The dissolved pellet was loaded onto the column and a 250 mL against 250 mL, 0.2–0.5 M KCl gradient was run. The repressor eluted after the gradient, and a wash of 300 mL of 0.5 M KCl was applied. The purified repressor was >95% pure as estimated from silver staining of an SDS–polyacrylamide gel. Each fraction containing TR was divided into 1-mL aliquots which were stored at −70 °C in the elution buffer (10 mM potassium phosphate, pH 7.6 with 0.5 M KCl). Protein concentrations were determined using an extinction coefficient of $1.45 \times 10^4$ cm$^{-1}$ M$^{-1}$ per monomeric subunit (Joachimiak et al., 1983).

*DNS Labeling.* Aliquots (1 mL) of purified TR were dialyzed against 1 L of 0.25 M potassium phosphate buffer, pH 8.3, for 3 h. Then 10 μL of a 0.02 M solution of dansyl chloride (Molecular Probes, Eugene, Oregon) was added to the solution of protein, and the reaction was allowed to proceed for 10 min. The solution was immediately applied to a Sephadex G-25 superfine column whose total volume was approximately 20 mL and which was preequilibrated with 10 mM phosphate, 10 mM KCl, and 0.1 mM EDTA, pH 7.6. The elution profile showed clear separation between the free dye band and the excluded protein. The latter was collected in approximately three fractions of 1 mL each. The most concentrated fraction was either used directly or dialyzed approximately 24 h either in the absence or in the presence of tryptophan (0.4 mM) against 1 L of 10 mM phosphate, 10 mM KCl, and 0.1 mM EDTA, pH 7.6, at 4 °C. The length of dialysis (or equilibration) of TR-DNS samples with tryptophan and without as a control was approximately 24 h because we noticed a slow time dependence to the equilibration of the samples with tryptophan over a 24-h period and subsequently acquired data after that period. No free dye, as observed by fluorescence intensity measurements, was found in the dialysis buffer. The ratio of probe to protein for the TR-DNS preparations was measured by taking the absorption spectrum between 250 and 500 nm. The spectrum showed two peaks, as expected, one centered at 280 nm corresponding to absorption from the protein and from the DNS label and one at 340 nm corresponding to absorption from the label alone. The labeling ratio (LR) was calculated using the method of Jameson (1978) as

$$LR = (A_{340}/E_{DNS340})/[[A_{280} - (1/2)A_{340}]/E_{prot280}]$$

*HPLC Size Exclusion.* DNS labeled and unlabeled TR were run on a 0.75 × 30 cm TSK 3000SW gel filtration column (Altex). A Beckman 420 HPLC system was used (Beckman Instruments, Palo Alto, CA), and elution profiles were measured by UV absorption at 280 nm. Pharmacia (Uppsala, Sweden) low molecular weight standards were used in generating a standard molecular weight line for the column. Samples (250 μL) of the standards and the TR and TR-DNS samples were loaded with concentrations in the range of 10–100 μM.

*Chymotrypsin Digests.* Chymotryptic digests of the labeled repressor were carried out following the method of Carey (1989). The enzyme was purchased from Boehringer-Mannheim (Indianapolis, IN). The products of the digest were analyzed by SDS–PAGE and silver stain and shown to be primarily the repressor with the six amino-terminal acids cleaved. The reaction mixture was applied to a Sephadex G-25 superfine desalting column, to separate the free peptide from the armless protein, and eluted with phosphate buffer (10 mM phosphate, 10 mM KCl, 0.1 mM EDTA, pH 7.6).

*Gel Retardation Assays.* Operator binding by the purified TR was ascertained by Yuan Ching Liu in the laboratory of K. S. Matthews using the gel retardation assay developed by Carey (1988) with a 40 bp synthetic DNA containing the *trp* EDCBA operator which has been shown to bind to the TR with similar affinity as the 90 bp fragment used by Carey (Chou & Matthews, 1990). The 26-mer containing the operator sequence was purchased in HPLC anion exchange purified form from Midland Reagents (Midland, TX) and labeled with $^{32}P$ for the gel mobility shift assays that were carried out under the same conditions as those above.

*Steady-State Fluorescence Measurements.* All fluorescence measurements were carried out in 10 mM potassium phosphate, 10 mM KCl, and 0.1 mM EDTA, pH 7.6, except for the Perrin plots in which the same buffer was used, but with no KCl. Steady-state measurements were performed on an ISS KOALA or an ISS GregPC (Urbana, IL) in analogue acquisition mode using a 300-W xenon arc lamp from ILC Technologies (Sunnyvale, CA). Steady-state polarization measurements on the TR-DNS samples were measured in L-format exciting at 350 nm with 8-nm bandwidth and using a Y460 cut-on filter (Hoya Optics, Freemont, CA) in emission or the monochromator set at 500 nm. Buffer background was subtracted for all samples, including those containing DNA, tryptophan (ICN Biomedicals, Cleveland, OH), and sucrose (Gold Label from Aldrich Chemical, Milwaukee, WI) at the same concentration as in the sample. Steady-state TR-DNS emission spectra were obtained using the same excitation optics but with an emission monochromator bandwidth of 8 nm. Steady-state TR intrinsic tryptophan polarization measurements were carried out using the 295-nm excitation from either the ILC lamp/monochromator combination or from the frequency doubled output of the Coherent 701 cavity dumped dye laser pumped with the modelocked Antares Nd-YAG laser also from Coherent (Palo Alto, CA). Emission spectra were obtained using the laser excitation at 295 nm and the emission monochromator with 8-nm band-pass. Again, buffer background was subtracted from each spectrum.

*Fluorescence Lifetime and Time-Resolved Anisotropy Measurements.* All time-resolved fluorescence measurements were carried out in 10 mM potassium phosphate buffer and 0.1 mM EDTA, pH 7.6. Lifetime and differential polarization measurements on TR-DNS were performed using the multifrequency phase/modulation acquisition electronics from ISS, Inc. (Urbana, IL) with the KOALA sample compartment or the multifrequency instruments described by Gratton and Limkeman (1983) and Piston and co-workers (1989). The excitation was from either an acousto-optically modulated Liconix He–Cd laser at 325 nm or externally pulse-picked output (355 nm) of the Coherent third harmonic generator (THG) coupled with the Coherent Antares mode-locked Nd–YAG laser. An external Bragg cell (model N13380 NEOS, Melbourne, FL) was driven with the Coherent cavity dumping electronics normally used in conjunction with the 700 series dye lasers. The diffracted beam was collected into an optical fiber model 77598 (Oriel Corp., Stratford, CT) and focused into the KOALA sample compartment with a 5-cm quartz lens. The cavity dumper was run in either divide by 10 or divide by 20 modes with base frequencies either near 2 or 4 MHz. Emission was monitored through a Y460 cut-on filter from Hoya Optics and compared to POPOP (Eastman Kodak, Syracuse, NY) with a lifetime of 1.32 ns in ethanol (Gratton et al., 1984). Lifetime measurements of the intrinsic tryptophan emission of TR were made using the harmonic content of the mode-locked laser/cavity dumped dye laser combination and a multifrequency fluorometer similar to that described by Alcala et al. (1985), as a function of emission wavelength with the ISA emission monochromator set at 320, 350, and 380 nm. In order to maximize signal as a function of decreasing protein concentration, dilution measurements as a function of frequency were made using a UV320 cut-on filter from Hoya Optics, or 320, 350, and 380 nm band-pass filters (Corion Corp, Holliston, MA) rather than the monochromator. Phase shift and modulation measurements of the TR samples were carried out with respect to the standard fluorophore, *p*-terphenyl in cyclohexane with a lifetime of 1.0 ns (Gratton et al., 1984). As a control for the fluorescence quenching experiments using potassium iodide, lifetime measurements were carried out as a function of NaCl concentration as well, and only a very small change (approximately 100 ps) in fluorescence lifetime was observed between 0 and 0.2 M NaCl.

*Data Analysis.* Multifrequency phase and modulation data were analyzed using the program Globals Unlimited (Urbana, IL). The fluorescence intensity decay was expressed as

$$I(t) = \sum_i \alpha_i e^{(-t/\tau_i)} \tag{4}$$

where $\alpha_i$ is the preexponential concentration factor and $\tau_i$ is the lifetime for the $i$th emitting component. The fractional contribution to the total fluorescence intensity, $f_i$, for the $i$th emitting component is related to its corresponding preexponential factor by

$$f_i = (\alpha_i \tau_i)/\sum_i \alpha_i \tau_i \tag{5}$$

The frequency response of the fluorophore is the Fourier transform of the intensity decay function, $I(t)$, where $G$ and $S$ are the real and imaginary parts of the transform, respectively:

$$G = \int_0^\infty I(t) \cos \omega t \, dt \tag{6}$$

$$S = \int_0^\infty I(t) \sin \omega t \, dt \tag{7}$$

The phase angle $\phi$, relative to excitation and the modulation ratio $M$, measured at frequency $\omega$ is related to the sine and cosine Fourier transforms of the fluorescence decay function, $S$ and $G$, (eqs 6 and 7) as follows:

$$\tan \phi = S/G \tag{8}$$

$$M = (S^2 + G^2)/I_{tot} \tag{9}$$

$$I_{tot} = \int_0^\infty I_t \, dt \tag{10}$$

where the sine and cosine transforms are related to the fluorescence lifetimes by

$$G = \sum_i \alpha_i \tau_i (1 + \omega^2 \tau_i^2)^{-1} \tag{11}$$

$$S = \sum_i \alpha_i \tau_i^2 (1 + \omega^2 \tau_i^2)^{-1} \tag{12}$$

With the global analysis software, multiple data sets for the magic angle lifetime experiments at differing wavelength, quencher, protein, or tryptophan concentration were analyzed simultaneously according to appropriate physical models for a consistent set of intensity decay parameters which describe all of the data surface in question. A full description of the current generation of fluorescence global analysis software can be found in Beechem et al. (1988).

Differential polarization data are related to the anisotropy decay through the relation between the sine and cosine

transforms of the parallel and perpendicular components of the emitted light, $I_{\parallel}(t)$ and $I_{\perp}(t)$, as in eqs 6 and 7 by

$$\Delta = \tan^{-1}(S_{\parallel}/G_{\parallel}) - \tan^{-1}(S_{\perp}/G_{\perp}) \quad (13)$$

and

$$\Lambda = \left[\frac{S_{\perp}^2 + G_{\perp}^2}{S_{\parallel}^2 + G_{\parallel}^2}\right]^{1/2} \quad (14)$$

where $\Delta$ and $\Lambda$ are the differential phase and modulation, respectively. The anisotropy decay, $r(t)$, is expressed as

$$r(t) = [I_{\parallel}(t) - I_{\perp}(t)]/[I_{\parallel}(t) + 2I_{\perp}(t)] \quad (15)$$

The physical model used to describe the anisotropy decay was that of a fluorophore attached to a macromolecule and undergoing depolarization through wobbling in a cone of half-angle $\theta_0$ (Kinosita et al., 1977; Lipari & Szabo, 1980) as well as due to the overall Brownian tumbling of the macromolecule. The mathematical expression for the fluorescence anisotropy decay assuming such a model is

$$A(t)/A_0 = A_{\infty}e^{(-t/\tau_{cp})} + (1 - A_{\infty})e^{(-t/\tau_w - t/\tau_{cp})} \quad (16)$$

where

$$A_{\infty} = [(1/2)\cos\theta_0(1 + \cos\theta_0)]^2 \quad (17)$$

and represents the anisotropy resulting from the steady-state distribution of dipoles, while the wobble correlation time $\tau_w$ is the time it takes after excitation to reach that distribution and $\tau_{cp}$ is the rotational correlation time of the protein.

An upper limit for the theoretical correlation time for a protein of a particular molecular weight and a prolate ellipsoidal shape with a particular axial ratio can be calculated using the relations presented by Steiner (1973), assuming that the probe dipole is oriented perfectly along the long axis of symmetry and assuming a very large hydration ($\delta_w$) of 0.5 g of $H_2O$/g of protein. First, the correlation time for a sphere of equivalent hydrated volume ($V_h$) is calculated as

$$\tau_{c(sphere)} = \eta V/RT \quad (18)$$

where

$$V_h = MW(V_p + \delta_w V_w) \quad (19)$$

Next, one calculates the ratio of the expressions for the correlation times for a sphere and for rotation about the short axis of the prolate ellipse as a function of the diffusion coefficients for those motions

$$\tau_{c(sphere)} = 1/6D_0 \quad (20)$$

$$\tau_{c(short\ ax)} = 1/6D_2 \quad (21)$$

$$\tau_{c(short\ ax)}/\tau_{c(sphere)} = D_0/D_2 \quad (22)$$

where $\tau_{c(sphere)}$ and $D_0$ are the correlation time and diffusion coefficient, respectively, for the spherical macromolecule, $\tau_{c(short\ ax)}$ is the correlation time for rotational motion about the short axis of the ellipse (end over end tumbling), and $D_2$ is the diffusion coefficient for rotation about that axis. The ratio of $D_2$ to $D_0$ for a macromolecule with an axial ratio $\gamma$ is calculated as

$$D_2/D_0 = (3/2)\gamma[(2\gamma^2 - 1)b - \gamma]/(\gamma^4 - 1) \quad (23)$$

and

$$b = (\gamma^2 - 1)^{-1/2}\ln[\gamma + (\gamma^2 - 1)^{1/2}] \quad (24)$$

and then used with eq 22 and the value of the correlation time of a sphere of the same volume to obtain the ratio of the theoretical correlation time around the short axis of a prolate ellipse.

## Results and Discussion

*Characterization of TR-DNS.* TR was purified and labeled as described under Materials and Methods. All of the dozens of preparations of TR-DNS which was have studied exhibited labeling ratios of 0.5–1 DNS moiety per dimer of TR. The labeling ratio is kept low in order to minimize the perturbation which the chemical modification makes on the system. To ascertain that the DNS label did not induce aggregation of the repressor, the unlabeled and labeled protein were tested in an HPLC size exclusion experiment. The unlabeled repressor at 10 $\mu$M loading concentration displayed an apparent molecular weight of 36 000, while the DNS-labeled repressor exhibited a similar value of 34 000. These values are slightly higher than those obtained by Joachimiak et al. (1983), 27 000–28 000 MW, using gravity gel permeation chromatography and by Arvidson et al. (1986) who obtained a value of 30 000 using HPLC with a TSK 250 column. In these studies, the concentration of the loaded protein and the dilution factor over the column were not reported. Because small zone exclusion chromatography is not an equilibrium technique, the loading concentration and volume, column volume, and elution time would exclude direct comparison of elution profiles for a dissociating oligomeric protein.

We also carried out a limited chymotrypsin digest of the DNS-labeled repressor following the methodology of Carey (1989) in order to determine if the DNS label was on the amino terminus of the repressor. Following the digest, the reaction mixture was applied to a Sephadex G25 superfine desalting column and eluted. The bulk of the fluorescence (>95%) was excluded from the column. SDS–PAGE with silver staining showed that the reaction cleaving the amino-terminal arm did take place and that the material excluded from the column and retaining the fluorescence was the arm-less repressor. Thus, the bulk of the DNS labeling is not on the amino terminus of TR.

The ability of the purified repressor to bind to a 40 bp oligonucleotide containing the *trp* EDCBA operator sequence was determined by the gel mobility shift assay described by Carey (1988). Our purified repressor exhibited a dissociation constant of approximately 0.6 nM, which is quite close to the 0.5 nM constant measured by Carey (1988), well within the error of the technique. DNS-labeled TR was also tested with the 40 bp fragment for its ability to bind to DNA. The dissociation constant measured for this modified protein was also 0.6 nM, indicating that the label had no significant effect upon the ability of TR to bind specifically to DNA. Finally the 26 bp synthetic operator used in these studies was tested with purified, unmodified TR, and the dissociation constant measured again by gel mobility shift assays was in the range of 1 nM. Due to the diffusion of the shorter DNA oligonucleotide away from the protein in the gel matrix as described by Carey (1991), the affinity for the 26-mer was estimated from the disappearance of the free DNA bond rather than the appearance of the complex band, since this showed up as a smear.

*Dilution Studies with DNS-Labeled Repressor.* In Figures 1a and 2a can be seen the anisotropy and multifrequency lifetime dilution data for TR-DNS in the absence and presence of the corepressor tryptophan at a concentration of 0.4 mM. These are the two fluorescence parameters needed for the calculation of an average correlation (tumbling) time for the macromolecule (see eq 2). It is quite clear from the plot of anisotropy versus protein concentration in Figure 1a that in

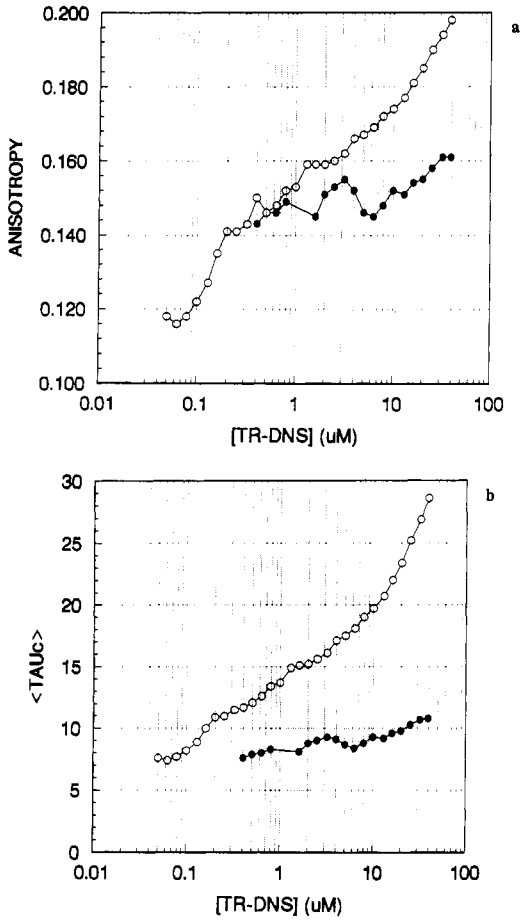


FIGURE 1: Steady-state dilution profiles of TR-DNS in the absence (open circles) and presence (closed circles) of 0.4 mM L-tryptophan. (a) Steady-state anisotropy values as a function of TR-DNS concentration. (b) Average rotational correlation times calculated using the steady-state anisotropy values in panel a and the average lifetimes calculated from interpolation of the average values obtained from the analysis of the multifrequency lifetime data for the same preparations using eq 2 and a limiting anisotropy value of 0.33. The buffer system was 10 mM potassium phosphate, 10 mM KCl, and 0.1 mM EDTA, pH 7.6.

absence of tryptophan (open circles) there is a marked dependence of the fluorescence anisotropy upon the concentration of the repressor protein, whereas this is not the case in presence of saturating corepressor. As described in the introductory section, the only interpretation of this result is that there is an oligomer dissociation reaction occurring upon dilution of the protein between approximately 40 and 0.04 $\mu$M dimer, whereas only a small degree of oligomerization is observed when the repressor is bound by tryptophan. While the dissociation reaction in absence of tryptophan is clearly observed, the exact shape of the profile can be affected by dissociation-dependent changes in the lifetime of the fluorophore. Simply stated, if the time scale of the emission process becomes shorter, there is less time for observation of the tumbling of the molecule and the measured anisotropy at a particular dilution is larger than it would be if no change in lifetime had occurred. As can be seen in Figure 2a, in the absence of tryptophan there is a small but detectable change in the multifrequency lifetime data as a function of the concentration of TR-DNS. The effect is slightly more pronounced when TR is bound by corepressor (Figure 2b), and the DNS lifetime is much shorter as evidenced by the shift to higher frequency of the phase and modulation frequency response curves. Multifrequency data similar to those in Figure 2a,b, but acquired for the same preparation as in Figure 1a, were analyzed

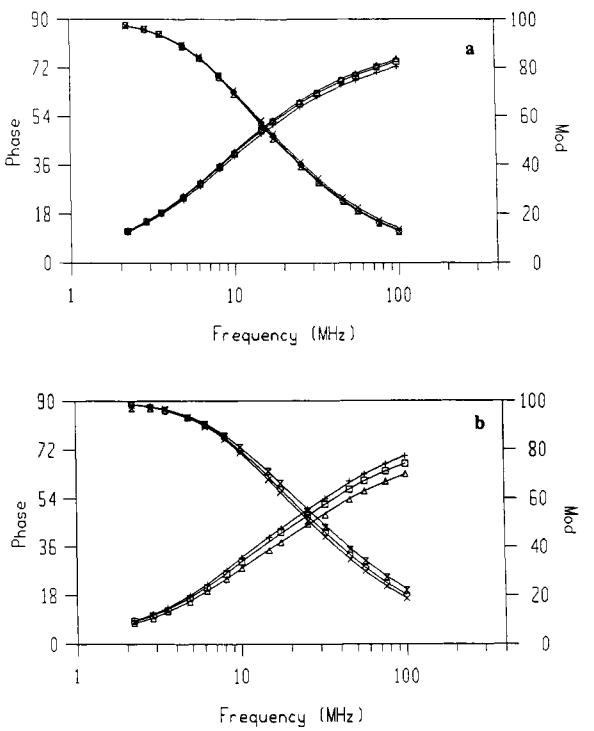


FIGURE 2: Frequency response profiles of the phase and modulation of TR-DNS as a function of protein concentration. (a) In the absence of tryptophan at 16 $\mu$M (open inverted double triangles, modulation; open triangles, phase), 4 $\mu$M (open circles, modulation; open squares, phase), and 1 $\mu$M (×, modulation; +, phase values) in TR-DNS expressed as dimer. (b) TR-DNS in the presence of 0.4 mM L-tryptophan at 18 mM (×, modulation; +, phase values), 6 $\mu$M (open circles, modulation; open squares, phase), and 2 $\mu$M (open inverted double triangles, modulation; open triangles, phase). Excitation was from the 325-nm line of an acousto-optically modulated He–Cd CW laser. Emission was monitored through a 1–42 cut-on filter. The excitation polarizer was set at the magic angle of 55° to eliminate rotational contributions to the decay. The buffer was the same as in Figure 2, except that no KCl was present.

Table I: Results of the Global Analysis of TR-DNS Lifetime Data[a]

| [TR-DNS] ($\mu$M) | [Trp] (mM) | $\tau_1$ (ns) | $\alpha_1$ | $\tau_2$ (ns) | $\alpha_2$ | $\tau_3$ (ns) | $\alpha_3$ | $\chi^2$ |
|---|---|---|---|---|---|---|---|---|
| 16 | 0 | 18.4 | 0.441 | 7.3 | 0.307 | 1.4 | 0.252 | 0.75 |
| 4 | 0 | 18.4 | 0.413 | 7.3 | 0.320 | 1.4 | 0.267 | 0.90 |
| 1 | 0 | 18.4 | 0.368 | 7.3 | 0.319 | 1.4 | 0.313 | 1.0 |
| 18 | 0.4 | 14.3 | 0.311 | 4.5 | 0.410 | 0.7 | 0.279 | 2.5 |
| 6 | 0.4 | 14.3 | 0.254 | 4.5 | 0.396 | 0.7 | 0.350 | 3.7 |
| 2 | 0.4 | 14.3 | 0.186 | 4.5 | 0.374 | 0.7 | 0.440 | 2.5 |

[a] The global $\chi^2$ in the absence of tryptophan was 0.82, while in the presence of tryptophan it was 2.56. Residuals in both cases were randomly distributed about zero.

as described under Materials and Methods using the Globals Unlimited software. As in other cases of DNS-labeled proteins (Royer et al., 1989, 1990), the TR-DNS decay fit well to a triple-exponential decay scheme, in which the lifetimes were linked for all concentrations, and their preexponential factors (or relative contributions) were allowed to vary. The values for the plots in Figure 2a,b are given in Table I. Those obtained for the preparation in Figure 1a are nearly identical and exhibit the same trends. Although the photophysics of DNS decay are not clearly understood, their sharp dependence upon the polarity of the environment render DNS quite useful in monitoring changes in the environment of macromolecules upon changing conditions. It has been demonstrated (Royer et al., 1989) that DNS in water is highly quenched whereas as the polarity of the solvent decreases, the DNS lifetime increases. The emission spectrum also shifts to higher energies

Table II: Results of the Analysis of TR-DNS Differential Polarization Data[a]

| [TR-DNS] ($\mu$M) | [Trp] (mM) | $\tau_{c1}$ (ns) | $\beta_1$ | $\tau_{c2}$ (ns) | $\beta_2$ | $\theta_0$ (deg) | $\chi^2$ |
|---|---|---|---|---|---|---|---|
| 16 | 0 | 43 | 0.59 | 0.29 | 0.41 | 33 | 2.8 |
| 4 | 0 | 37 | 0.53 | 0.35 | 0.47 | 36 | 1.9 |
| 1 | 0 | 32 | 0.48 | 0.48 | 0.52 | 30 | 2.2 |
| 18 | 0.4 | 29 | 0.35 | 0.32 | 0.65 | 46 | 2.7 |
| 6 | 0.4 | 28 | 0.32 | 0.33 | 0.68 | 48 | 3.4 |
| 2 | 0.4 | 34 | 0.25 | 0.12 | 0.75 | 52 | 2.0 |

[a] Single curves were analyzed and residuals were randomly distributed about zero. The lifetimes used in the analysis were those above, and $A_0$ was 0.33.

(blue) with decreasing polarity. The triple-exponential decay observed for DNS bound to macromolecules is thought to arise both from solvent-induced heterogeneity of the electronic states of the DNS (Lambooy et al., 1982; Guest et al., 1992), as well as the intrinsic dynamically based heterogeneity of fluorophores in macromolecules (Alcala et al., 1987). Changes in the environment of the DNS probe which are dependent upon the protein concentration, regardless of their photophysical origin, are necessarily due to changes in the oligomeric state of the molecule.

For the purposes of calculating the average correlation time (changes in which are related to the tumbling and thus size of the molecule), the fractional contribution of each lifetime component was used to calculate the average fluorescence lifetime of the probe as a function of concentration. Values were interpolated between the averages calculated from data obtained using the preparations used in Figure 1a at two concentrations, 18 and 1 $\mu$M dimer, and these average lifetimes and the anisotropy values in Figure 1a were used to calculate the average correlation time of the TR-DNS as a function of its concentration. The average correlation time calculated from the steady-state anisotropy values and the average lifetime values is plotted versus concentration in Figure 1b for TR-DNS in the absence of tryptophan (open circles). The same type of experiment and analysis was carried out for TR-DNS in the presence of tryptophan. The anisotropy profile is shown in Figure 1a, and the average correlation times are shown in Figure 1b (closed circles). As in the case of the raw anisotropy data, there is very little dependence of the average rotational correlation time on the concentration of the protein in the presence of tryptophan whereas a large decrease in correlation time as a function of dilution is observed for the aporepressor. The largest effect of the lifetime correction is to shift the curve in presence of tryptophan down with respect to the aporepressor such that the values at high concentrations in the presence of tryptophan are much lower than those in its absence, and the two plots tend to converge at a lower concentration of repressor. We conclude from these observations that, in the absence of tryptophan, the repressor undergoes an oligomerization interaction upon increasing the protein concentration and that the binding of corepressor highly disfavors this association.

In Figure 3 are time-resolved fluorescence anisotropy data for TR-DNS as a function of repressor concentration in the absence and presence of tryptophan. The lifetime values and preexponential factors were those recovered from the global analysis of the lifetime data in Figure 2a,b and were fixed parameters in the analysis of the differential polarization. The multifrequency differential polarization data for TR-DNS equilibrated overnight either in the absence or presence of tryptophan were analyzed using a model in which the multiple lifetime species undergo independent local and global rotational motion. The global rotational motion was modeled to be an

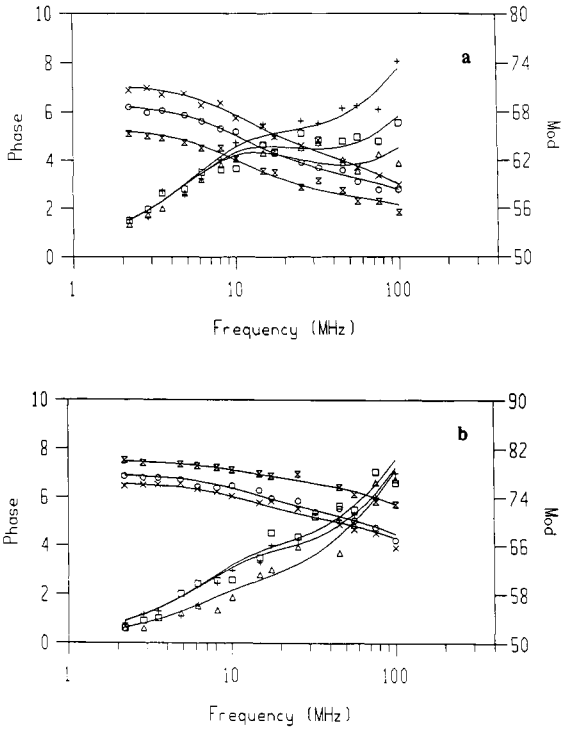


FIGURE 3: Frequency response profiles of the differential phase and modulation data for TR-DNS as a function of protein concentration expressed as dimer. (a) In the absence of tryptophan at 16 $\mu$M (open inverted double triangles, modulation; open triangles, phase), 4 $\mu$M (open circles, modulation; open squares, phase), and 1 $\mu$M (×, modulation; +, phase values). (b) In the presence of 0.4 mM L-tryptophan at 18 $\mu$M (×, modulation; +, phase values), 6 $\mu$M (open circles, modulation; open squares, phase), and 2 $\mu$M (open inverted double triangles, modulation; open triangles, phase). Excitation was from the 325-nm line of an acousto-optically modulated He–Cd CW laser. Emission was monitored through a 1–42 cut-on filter. The buffer was the same as in Figure 2, except that no KCl was present.

average value resulting from a mixture of oligomers in solution, while the local motion was modeled as a wobbling in a cone of half-angle $\theta_0$ (Kinosita et al., 1977; Lipari & Szabo, 1980). The results of the analysis are given in Table II. The local motion was approximately 120–480 ps and in agreement with observations of DNS rotations on a number of macromolecules (Royer, unpublished results; Guest et al., 1991). The overall contribution of the first local rotation in the total depolarization increased both upon protein dilution and upon addition of tryptophan, indicating more freedom of motion of the probe under these circumstances (see Table II). The global macromolecular rotational rate was taken to be an average of the different oligomeric species in solution. The fits to both data sets were good and confirm that, in the absence of corepressor, dilution of TR-DNS leads to dissociation of an oligomeric form of TR larger than dimer. In the absence of corepressor, the average global correlation time decreases from 43 to 37 to 32 ns over the concentration range studied (16–1 $\mu$M TR, expressed as dimer). In the presence of tryptophan, no significant trend in the concentration dependence of the global tumbling was observed, and the value of the correlation time was in general, lower than that observed in the absence of corepressor. In the presence of corepressor, the value at the highest concentration (18 $\mu$M TR) is 29 ns, much lower than that observed in its absence at the high concentration. It remains approximately constant at 28 ns upon dilution to 4 $\mu$M dimer. Only the lowest concentration yielded inconsistent results, with a small increase in the global correlation time to 34 ns. The parameters recovered from single-curve analysis of time-resolved anisotropy data in complex systems are generally highly

Table III: Results of the Perrin Plots on TR-DNS

| [TR-DNS] ($\mu$M) | [Trp] (mM) | $A_{oapp}$ (intercept) | $V_h \times 10^{-3}$ (cm$^3$/mol) | $\tau_{cp}$ (ns)[a] |
|---|---|---|---|---|
| 16 | 0 | 0.255 ± 0.005 | 81 ± 6 | 32.3 ± 2.4 |
| 4 | 0 | 0.232 ± 0.005 | 69 ± 6 | 27.7 ± 2.2 |
| 1 | 0 | 0.214 ± 0.008 | 61 ± 8 | 24.5 ± 3.2 |
| 18 | 0.4 | 0.180 ± 0.006 | 45 ± 5 | 18.1 ± 2.0 |
| 6 | 0.4 | 0.175 ± 0.008 | 34 ± 5 | 13.7 ± 2.1 |
| 2 | 0.4 | 0.153 ± 0.010 | 36 ± 9 | 14.5 ± 3.7 |

[a] $\tau_{cp}$ corresponds to the correlation time of the protein and is referred to as $\tau_{cl}$ in Table II.

correlated, and one must use caution in their interpretation. The lifetime changes in absence of tryptophan were small, and the anisotropy changes were large. In addition, the correlation times due to tumbling contributed at least 50% to the total depolarization and were well separated from those arising from local probe motion. In this case it is clear that the changes observed in the raw differential polarization data arise from changes in the global tumbling time and can be reasonably interpreted as a shift toward a smaller oligomeric state upon dilution. In the presence of tryptophan, the lifetime is shorter and thus less sensitive to global tumbling. The changes in lifetime are larger, and the values of the global tumbling times contribute less to the overall depolarization. Values of the wobble angle above 50°, the value obtained in the presence of tryptophan, indicate that the model is near its limits of applicability (Kinosita et al., 1977). For these reasons, the correlation times for the global macromolecular tumbling recovered from the differential polarization data obtained in the presence of tryptophan may be less reliable than those obtained in its absence.

Because of the inherent uncertainty in time-resolved anisotropy parameters recovered from the analysis of data from complex systems, an additional characterization of the protein and tryptophan concentration dependence of the macromolecular size of TR-DNS was performed. The results of Perrin sucrose titrations of TR-DNS equilibrated overnight with or without tryptophan are shown in Figure 4a,b. In Figure 4a, the protein concentration dependence of the Perrin plot for TR-DNS in the absence of tryptophan at 16, 4, and 1 $\mu$M TR-DNS dimer is shown. The data in Figure 4b correspond to Perrin plots obtained with 18, 6, and 2 $\mu$M TR-DNS in the presence of 0.4 mM tryptophan. The linear regressions of the Perrin plots yielded best-fit slopes of the line which were used along with eq 3 to calculate the apparent molecular volume of the repressor. In these fits, the weighted contribution of the three fluorescence lifetime components to the average anisotropy were taken into account following the method of Gratton, which is documented by Fernando (1991). The results of the fits are given in Table III. It can be seen from Figure 4 and Table III that the slopes and the calculated molecular volumes in the absence of tryptophan are significantly larger than those observed in its presence and that, moreover, they exhibit a strong concentration dependence. The value of the molecular volume in absence of tryptophan decreases from 81 000 to 61 000 cm$^3$/mol between 16 and 1 $\mu$M TR-DNS dimer. The corresponding correlation times, also given in Table III, are smaller than those obtained from the time-resolved experiments but show the same trend, decreasing from 32.5 to 24.5 ns over the concentration range of 16–1 $\mu$M. In the presence of tryptophan, as in the case of the time-resolved anisotropy experiments, the molecular volumes from the Perrin plots are much smaller than in the absence of tryptophan and show a smaller overall decrease from 45 000 to 18 $\mu$M to 36 000 cm$^3$/mol at 2 $\mu$M dimer. Likewise, the

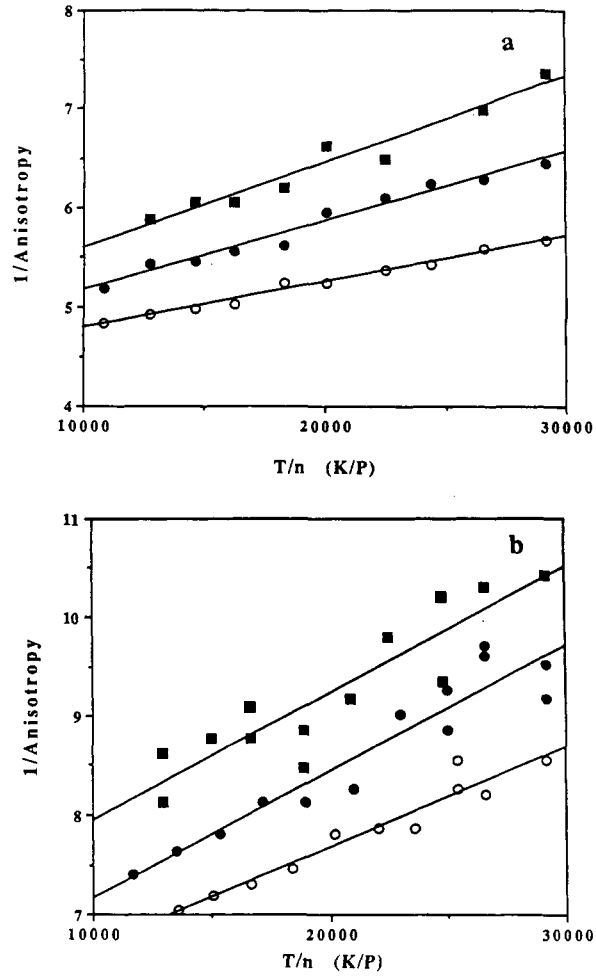


FIGURE 4: Perrin plots of TR-DNS as a function of protein concentration. (a) TR-DNS in the absence of tryptophan as 16 $\mu$M (open circles), 4 $\mu$M (closed circles), and 1 $\mu$M (closed squares). (b) TR-DNS in the presence of 0.4 mM tryptophan at 18 $\mu$M (open circles), 6 $\mu$M (closed circles), and 2 $\mu$M (closed squares). Excitation was at 340 nm with a xenon arc lamp and 8-nm band-pass, and emission was monitored with both a 1–42 cut-on filter and an ISA monochromator set at 500 nm with an 8-nm band-pass. The buffer was the same as in Figure 2, except that no KCl was present.

correlation times are smaller, decreasing from 18.1 to near 14 ns from 18 to 2 $\mu$M in TR-DNS. These data are in agreement with the steady-state single viscosity dilution profiles and the time-resolved anisotropy data which indicate that *trp* repressor undergoes a subunit association reaction over the range studied and that addition of corepressor shifts this equilibrium to the lower molecular weight form of the repressor. The lower overall values or the correlation times for global molecular tumbling obtained from the Perrin plots as compared to the correlation times recovered from the time-resolved data reflect either a contribution of the local motion to the Perrin plot slope or the inherent uncertainty in the model used for analysis of the time-resolved data. We also point out that the intercept of the Perrin plots yields apparent limiting anisotropy values which decrease both upon dilution and upon tryptophan binding. This indicates, as in the case of the time-resolved experiments, that corepressor binding and dilution both result in an increase in the local mobility of the DNS probe.

Although there is some difference in the actual values obtained by these last two method, it is clear that an oligomerization equilibrium is being monitored and that the addition of tryptophan shifts the equilibrium toward a lower molecular weight species. The results are in good agreement with the steady-state dilution profiles in Figure 1a,b, indicating that

the small difference in salt concentration (0–10 mM) has no great effect either on the lifetimes or the correlation times. In fact, the time-resolved anisotropy experiments were repeated in the buffer containing 10 mM KCl at 18 and 1 $\mu$M in TR-DNS, and the results were nearly identical to those obtained from the analysis of the data in Figure 3a,b with the same protein concentration dependent decrease in global correlation time observed in the absence of tryptophan and not in its presence.

Due to the fact that hydration and shape, as well as size, contribute to the frictional resistance to rotational diffusion, the existence of oligomerization equilibria can be detected with great accuracy in by fluorescence anisotropy, but these experiments rarely allow for the unambiguous identification of the stoichiometries of the various species involved. Nonetheless, a comparison of the correlation times obtained in our experiments with those which one can calculate theoretically provides a means for estimating the stoichiometries to which the observed oligomerization equilibria may correspond. One can calculate an upper limit for the theoretical rotational correlation time for a dimeric protein of 26 000 MW which can be approximated by a prolate ellipse exhibiting (as does TR) an axial ratio of 1.7 (Schevitz et al., 1985). This upper limit calculation is carried out as described under Materials and Methods. We assume that the specific volume of the protein, $V_p$, is 0.73 cm$^3$/g and that the specific volume of the water is 1 cm$^3$/g. From these relations, we obtain a value for the correlation time of a spherical protein of MW 26 000 which would be 13 ns. Next, one calculates the theoretical correlation time which would be observed if the fluorophore rigidly attached to a macromolecule with a prolate ellispoidal shape of axial ratio of 1.7 and if the fluorophore's emission dipole were perfectly aligned with the long axis of the ellipse. Because this theoretical calculation assumes a rigidly attached fluorophore aligned along the long axis and very high hydration, this correlation time truly represents an upper limit for the actual value. The ratio of correlation times (sphere/short axis) for TR is calculated to be 1.3. Thus, the longest correlation time which could be observed for dimeric TR would be 16.9 ns. The values observed experimentally for TR-DNS in the absence of corepressor are all higher than this upper limit calculation. It is quite clear that TR forms an oligomer which is larger than dimer. The dilution profiles are indicative of an equilibrium which includes dimers and tetramers and perhaps higher order oligomers. In fact, the 43-ns value obtained from the analysis of the time-resolved data and even the 32.5-ns value obtained from the Perrin plot data (both at 16 $\mu$M in TR-DNS dimer) are at least twice the theoretical upper limit value for the dimer. The large values of the correlation times may be partially due to formation of end-to-end elongated tetramers which would be highly asymmetrical (with a 4:1 axial ratio) and thus exhibit an unusually long correlation time. Moreover, the concentration at which the longest correlation times were observed, 16 $\mu$M, is in the middle of the range of the anisotropy dilution curve (Figure 1). In fact, the dilution profile of apo-TR in Figure 1 extends for 3 log units with no clear plateaus, particularly at the high concentration end of the profile. This strongly indicates that the equilibrium may involve more than two oligomeric species and that the repressor forms higher order oligomers. Kumamoto et al. (1987) report binding of 2–3 tandem repressors to various DNA oligomers containing the operator sequences, and Otwinowski et al. (1988) suggest that the amino-terminal arms of the repressor may play a role in stabilizing the tandem binding. In the presence of DNA, Carey (1988) showed that very large stoichiometries of protein/DNA complexes were observed under certain conditions (more than enough for a complete coating of the DNA with protein) and that protein–protein interactions must therefore be implicated. Whether the observed oligomerization equilibrium is a simple dimer–tetramer interaction or whether higher order species are involved, it is clear from the present data that in the presence of corepressor the oligomerization is strongly shifted in favor of the dimeric species. The values of the correlation times obtained from the Perrin plots in the presence of tryptophan at the two lowest concentrations (approximately 14 ns) are in good agreement with that expected for a dimer (<16.9 ns). Those obtained from the time-resolved data were higher, but, as pointed out earlier, the fraction of depolarization due to local motion yielded wobbling angles which were at the limit of applicability of the model.

The time-resolved studies also yield information concerning the conformational changes brought about by dilution and tryptophan binding. In all cases, there is a nonnegligible contribution to the depolarization by local flexibility of the DNS probe, consistent with our conclusion that the average correlation times in Figure 1b result from a combination of the local and global tumbling and thus are much lower than the actual global macromolecular rotational correlation time. Second, both the oligomer dissociation and the binding of the corepressor result in a decrease in the fluorescence lifetime of the DNS probe as well as an increase in the contribution of the local rotational motions to the overall depolarization of fluorescence. The emission spectrum of the TR-DNS shifts significantly to the red in presence of tryptophan. In the case of DNS, this quenching of the fluorescence lifetime and the red-shift in emission can be correlated with a greater exposure to the solvent (Royer et al., 1989). A greater exposure to solvent is also consistent with an increase in local rotational mobility. It is not unexpected for an oligomer dissociation reaction to lead to greater solvent accessibility of residues in the protein. And clearly, although the repressor structure generally becomes more compact upon tryptophan binding (Schevitz et al., 1985; Zhang et al., 1987), it is not necessarily contradictory that the environment immediately near the DNS label position(s) could change in such a manner that the DNS label becomes more exposed to solvent when repressor binds. This is particularly true since tryptophan binding induces oligomer dissociation, and the red-shift, decrease in lifetime, and increase in rotational rate may be a direct consequence of tetramer dissociation, rather than a tertiary conformational change in the local DNS environment.

*Dilution Studies of Native Repressor.* We also measured the intrinsic tryptophan anisotropy dilution profile of the native repressor, and this is shown in Figure 5a. This profile, which exhibits a protein concentration dependent decrease in the fluorescence anisotropy in the concentration range of 60–1 $\mu$M dimer, is quite consistent with the results from the DNS-labeled repressor and confirms the protein subunit association equilibrium over this range. Since no clear plateau at low concentrations was observed in either the native TR or the TR-DNS anisotropy dilution profiles, we examined the intrinsic fluorescence emission energy in the absence of tryptophan because this observable parameter can be detected at lower concentrations. Trp 19 is found at the interface between two monomeric subunits. Tasayco and Carey (1992) using chymotryptic digestion and Mann and Matthews (personal communication) using site-directed mutagenesis have shown that this tryptophan is responsible for 80–90% of the fluorescence emission intensity. Time-resolved potassium

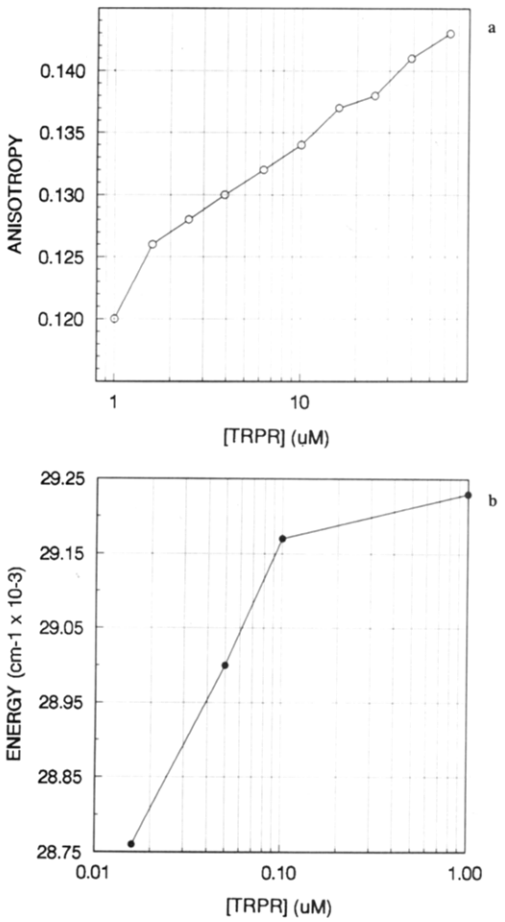


FIGURE 5: Dilution profiles of unlabeled TR using (a) the intrinsic fluorescence steady-state anisotropy and (b) the intrinsic average emission energy. Excitation was at 295 nm with a xenon arc lamp in panel a and a Nd–YAG/R6G double dye laser in panel b. Emission was monitored through a monochromator with 8-nm band-pass and set at 340 nm in panel a. The buffer was the same as in Figure 1.

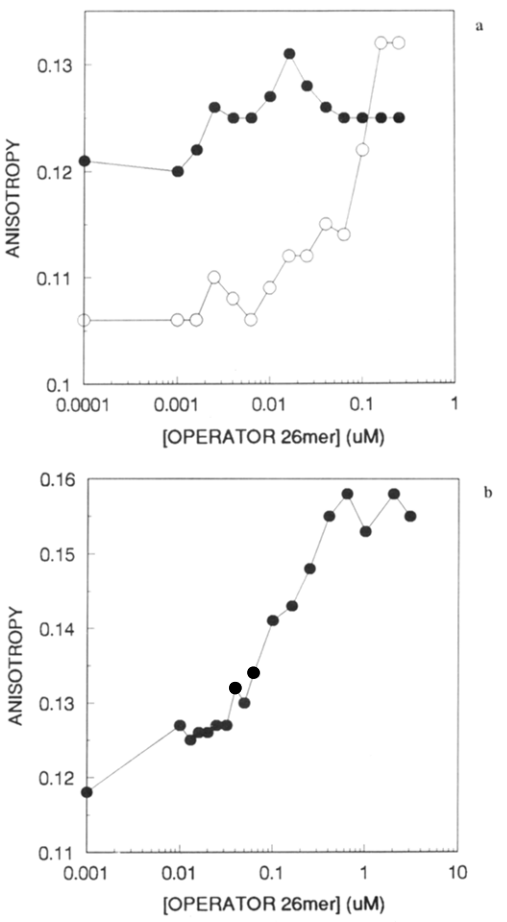


FIGURE 6: Operator 26-mer titrations of (a) TR-DNS at 0.2 $\mu$M in dimer in the presence (open circles) and absence (closed circles) of 0.4 mM L-tryptophan monitoring the steady-state anisotropy of the DNS emission. Excitation was at 340 nm, and emission was monitored through a 1–46 cut-on filter. (b) Unlabeled TR at 1 $\mu$M dimer with no tryptophan present monitoring the steady-state anisotropy of the intrinsic tryptophan emission of the repressor. The excitation wavelength was 295 nm, and emission was monitored at 345 nm. The buffer was the same as in Figure 1.

iodide quenching experiments (data not shown) have indicated that the longest lifetime component of the repressor emission can be assigned to Trp 19.

Given this framework, assuming that Trp 19 was blue and quite buried near the dimer interface and moreover responsible for most of the intrinsic fluorescence of the repressor, we expected that, upon dimer dissociation, if that occurred with dilution, we would observe a red-shift in emission. A dilution profile of the emission energy (lower energy = redder spectrum) of TR is shown in Figure 5b. For this preparation, no significant change in emission energy occurs until dilutions below 100 nM. Between 100 and 16 nM there is a 400 wavenumber decrease in the emission energy, which is a quite significant shift. Since no plateau is reached, we cannot give an absolute value for the dissociation constant; but assuming that 10–90% of the dissociation from dimer to monomer should take place over 2.3 log units, we estimate the dissociation constant for this preparation to be in the nanomolar range. Given the range of concentration of the repressor in vivo, 0.1–0.8 $\mu$M dimer, we do not expect that this monomer–dimer equilibrium has any biological significance. However, since its affinity appears to be in the range of DNA binding affinity, it could have some influence on the measurement of the specific DNA binding constant. Since the corepressor should stabilize the dimer, the affinity of the holorepressor dimer should be higher than that of the aporepressor. Although the DNA binding profiles of Carey (1988) in gel retardation assays show no evidence for cooperativity, those of Hurlburt and Yanofsky (1990) using filter binding techniques show a marked cooperativity of binding. This high affinity between the subunits is consistent with observations by Yanofsky and co-workers (Graddis et al., 1988) that, using concentrations between 25 and 50 $\mu$M dimer (>10 000-fold above our estimated $K_d$), heterodimer formation only occurs at temperatures near 65 °C. It is also consistent with the extensive contacts observed in the interlocked helical subunit interface structure of the repressor (Zhang et al., 1985).

*Operator DNA Binding Studies.* The ability of fluorescence anisotropy measurements to monitor changes in the size of molecular complexes was used to study the binding of the repressor to the 26-mer containing the *trp* EDCBA operator sequence. These studies were carried out both with the native and DNS-labeled repressor and in the presence of tryptophan in the latter case. The results of the titrations of the labeled protein, at a fixed concentration of 0.2 $\mu$M dimer, with the operator DNA fragment are shown in Figure 6a in the absence (closed circles) and presence (open circles) of 0.4 $\mu$M tryptophan. In the absence of co-repressor, only a small increase in anisotropy is observed, and this occurs at very low 26-mer concentration, <10% of the total protein concentration. In the presence of co-repressor, the titration anisotropy curve is similar to that observed in the absence of co-repressor at low DNA 26-mer concentration, but then a significant increase in anisotropy is observed between approximately 0.05 and 0.2

μM 26-mer. It would appear that both in the absence and presence of co-repressor and at low 26-mer concentration, binding of oligomers of TR-DNS is observed, giving rise to the apparent high stoichiometries, as approximated by the concentration ratios and the total anisotropy changes. In the presence of tryptophan, as more 26-mer becomes available for binding, one observes the formation of TR/DNA complexes with a stoichiometry of one dimer per 26-mer operator fragment. In this case, binding is within the stoichiometric rather than equilibrium binding limit, as would be expected at a concentration of protein which is approximately 500-fold the measured specific complex $K_d$ of 0.5 nM (Carey, 1988). In the absence of tryptophan, only a fraction of the total anisotropy change observed in the presence of tryptophan is evident (approximately 30%), and it occurs at an operator concentration which is less than 10% of the dimer concentration. Addition of further operator cannot drive the binding reaction, because the protein which is binding to the DNA as an oligomer is not at a high enough concentration. Under these conditions, the oligomeric form of the repressor which binds nonspecifically is disfavored.

In Figure 6b, the intrinsic tryptophan anisotropy of 1 μM unlabeled TR is monitored as a function of 26-mer operator concentration. Binding is observed over 1 log unit, and it can be seen that 50% of the total change in anisotropy is observed at a DNA 26-mer concentration which is much less than 50% of the TR dimer concentration (0.13 μM operator compared to 1 μM DNA). In addition, there is an increase in anisotropy from that observed for the TR alone upon the addition of only 1 nM operator fragment. These observations are highly indicative of the binding of oligomers of TR to the 26-mer. At the high concentration plateau of the titration curve, the concentration of DNA is approximately equal to half the TR dimer concentration. If one assumes that, at the top of the anisotropy curve, all of the protein is bound, then the stoichiometry of the complexes would be two dimers (i.e., one tetramer) per operator 26-mer. Since the total protein concentration is higher than in Figure 6a, a greater degree of association of the protein to the DNA can be achieved by increasing the DNA concentration because the protein–protein interactions necessary to the nonspecific complexes are favored. Although the stoichiometries of the complexes can only be estimated from our observations (anisotropy profiles can be influenced if there are many complexes with different stoichiometries), the simple comparison of the range of operator concentrations over which the changes in anisotropy occur with the concentration of the protein in each experiment constitutes conclusive evidence that the repressor can bind to the 26-mer operator fragment in the form of an oligomer of higher order than dimer in the absence of tryptophan. In the presence of tryptophan, this is only observed when the concentration of 26-mer is limiting. We also point out that only small changes in the intensities of the emission were observed in these experiments confirming that the bulk of the aniostropy changes are a direct consequence of the increase in the size of the macromolecule when the protein binds to the DNA. These results are in agreement with the observations of Carey (1988) using tritiated protein and $^{32}$P-labeled operator fragments which demonstrated stoichiometries in excised gel shift bands which corresponded to up to four dimers per 28 base pairs and imply quite extensive protein–protein interactions in addition to protein–DNA interactions. These severely retarded gel shift bands were observed under conditions of very low DNA concentrations (<10 pM) and relatively high protein concentrations (>0.1 μM TR dimer) both in the absence and presence of tryptophan. Our conditions for the data in Figure 6a use protein concentrations similar to those where Carey (1988) observed the higher order complexes (0.2 μM TR dimer), but we use much more DNA (0.001–3 μM). Thus, in the presence of tryptophan, there is enough DNA present in our case such that all of the protein dimers can take part in a specific dimer/operator complex. In the gel mobility shift assays of Carey (1988), the DNA concentration was limiting and the ratio of protein to DNA in the presence of tryptophan was a factor of 10 000. Therefore, stoichiometries of the gel shift bands exceeded one dimer/28 base pairs when the protein concentration was raised above 100 nM even in presence of the corepressor. In the absence of tryptophan, we observe binding at DNA concentrations well below the concentration of protein, indicating that higher order oligomers bind in absence of tryptophan. Carey also reported high stoichiometries in the gel shift bands in the absence of corepressor and at protein concentrations above 100 nM. In comparing our results with the gel mobility shift experiments, one must remember that, in the latter, the observable signal is due to the *DNA* (at very low concentrations), whereas, in the present experiments, the observable signal is due to the *protein*. Carey observed that at 100 nM dimer, both in the absence and presence of corepressor, much of the DNA (<10 pM) was in complexes that were severely retarded in the gel shift. On the other hand, in the present experiments a significant change in the anisotropy signal is observed only when a significant proportion of the total protein is involved in complexes with DNA. Taking this into account, the anisotropy titrations presented here are quite consistent with Carey's gel mobility shift experiments and further demonstrate that both the stoichiometries and the degree of association of *trp* repressor with DNA are an intricate function of the DNA, protein, and tryptophan concentrations.

## Conclusions

A number of points can be made concerning our fluorescence anisotropy results. First, TR-DNS in the absence of tryptophan displays a marked oligomer association from 40 nM to 40 μM, and the correlation times and volumes are consistent with a predominantly tetramer–dimer equilibrium with perhaps formation of some higher order oligomers. Secondly, in the presence of the corepressor there is very little protein concentration dependence of the anisotropy and thus oligomeric state over the concentration range studied, and the correlation times and volumes are consistent with a tryptophan-induced shift of the equilibrium toward dimeric repressor. Thus, there is an allosteric energetic linkage between corepressor binding and the tetramer–dimer equilibrium.

The DNA binding anisotropy profiles indicate that the corepressor-bound form of the protein binds as a dimer to its cognate DNA sequence, whereas in the absence of corepressor, tetramers and higher order oligomers can bind to the DNA. These observations are in agreement with those of Carey (1988), Gunsalus and co-workers (Bass et al., 1987; Kumamoto et al., 1987) and Muller Hill (Staake et al., 1990), who observed that more than one dimer could bind to various operator sequences when the protein concentration was near 100 nM dimer. Gunsalus and co-workers (Kumamoto et al., 1987) point out that intracellular concentrations of the repressor are relatively high and are in the range of the tandem binding such as they observed in vitro. They suggest that these interactions may thus have biological significance.

The tetramer (or higher order oligomer)–dimer equilibrium and the high stoichiometries of the protein–DNA complexes observed in the absence of the corepressor along with the

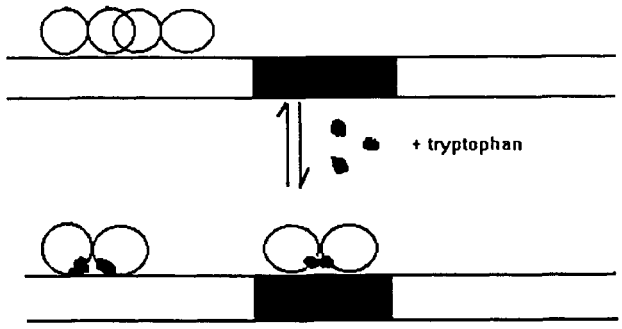


FIGURE 7: Schematic representation of a model for how the protein and tryptophan concentration-dependent competition between protein–protein interactions and different modes of protein–DNA interactions can combine with the excess of nonspecific DNA to efficiently regulate the transcription of the *trp* EDCBA genes. In the absence of tryptophan and at relatively high concentrations of repressor (near 1 $\mu$M), the protein–protein interactions are favored in the nonspecific binding mode. In addition, the large excess of nonspecific DNA aids in keeping the specific operator site unoccupied. However, in the presence of tryptophan, these protein–protein interactions are highly disfavored, and, in addition, the conformation of the repressor when bound by tryptophan leads to a 200-fold higher affinity for its cognate sequences. This leads to occupation of the specific sites, including that upstream of the gene for TR. This autorepression would serve to keep the protein concentration relatively low (near 0.1 $\mu$M), further disfavoring the protein–protein interactions involved in the nonspecific complexes.

profound effect of the corepressor on these equilibria lead us to propose that the tryptophan-mediated switch between active and inactive repressor involves destabilization by the corepressor of the higher order protein–protein interactions. We propose an in vivo model (Figure 7) in which, with no tryptophan in the growth medium, the repressor, which is at a relatively high concentration (800 nM dimer; Gunsalus et al., 1986), is bound to nonspecific DNA as a tetramer (or higher order oligomer). When tryptophan is added to the medium, it binds to the repressor and destabilizes the subunit interactions involved in the nonspecific complex in favor of the specific dimeric complex which is active in repressing transcription. This allosteric coupling of tryptophan binding with the protein subunit interactions would also provide a rationale for why TR represses its own transcription in presence of tryptophan, leading to a near 10-fold decrease in the cellular concentration of the repressor (Gunsalus et al., 1986). In the discussion of her results, Carey (1988) points out that the specificity ratio for the *trp* repressor is only 200 and suggests that there may be additional factors which increase the specificity ratio in vivo. We suggest here that, in the absence of tryptophan, and thus at relatively high concentrations of TR, the competition by protein–protein interactions, in addition to the large excess of nonspecific DNA over the cognate sequences, would combine to leave the operator sequences largely unoccupied, and transcription would take place. However, with increases in tryptophan concentration, these competing protein–protein interactions are destabilized. Since tryptophan binding also results in changes in the TR tertiary conformation leading to the 200-fold change in affinity for the specific sequence, the operator sequences are largely occupied and transcription is repressed. This increased repression eventually results in autorepression, thus decreasing the repressor concentration itself, which while remaining well above the specific binding mode dissociation constant, highly disfavors the protein–protein interactions of the nonspecific binding mode. The above model illustrates how the thermodynamic relationships between ligand binding and protein–protein interactions could provide an additional level of discrimination between specific and nonspecific DNA binding modes and how coordinated changes in both tryptophan and repressor concentration could lead to efficient transcriptional regulation.

The *trp* repressor is only one of a larger number of DNA-binding proteins in which the interactions between polypeptide chains play a significant role. It would be highly informative to apply the fluorescence spectroscopic techniques presented here toward investigating the equilibrium thermodynamics of protein–protein interactions and their role in DNA binding for a number of important eukaryotic transcriptional regulatory proteins. Competition between dimerization partners in the HLH-type proteins is at the crux of developmental control in mammalian myogenesis (Weintraub et al., 1991; Benezra et al., 1990). Control by competition for dimerization is involved in *Drosophila* development and apparently in cell transformation by the c-*myc* oncogene products, although the nature of the regulatory role of the proteins which bind to c-*myc* and the DNA sequences which are targeted has yet to be established (Blackwood & Eisenman, 1991; Prendergast et al., 1991). Hormone receptors are another class of transcriptional regulators in which protein–protein interactions in addition to protein–ligand interactions modulate DNA-binding properties (Diamond et al., 1990). The list of eukaryotic transcription factors whose functionality is directly linked to protein–protein interactions is rapidly growing. Using the bacterial model system, the tryptophan repressor protein, we have demonstrated that the energetic role of subunit interactions can be readily probed by fluorescence spectroscopic methods. Because fluorescence is a relatively straightforward solution methodology, the effect of solution conditions such as ligand concentration, salt, pH, and temperature upon protein–protein and protein–DNA interactions can be easily ascertained. In addition to structure, the characterization of the energetics of macromolecular complexes is fundamental to the understanding of their function. The application of fluorescence spectroscopic methodologies to such DNA-binding proteins as mentioned above would certainly lead to a deeper general understanding of transcriptional regulation.

## ACKNOWLEDGMENTS

Some of the data were obtained at the Laboratory for Fluorescence Dynamics, which is a national research resource center jointly funded by the National Institutes of Health and the University of Illinois at Urbana-Champaign. We thank Dr. Kathleen Shive Matthews for the plasmid and bacterial strain used to overproduce the repressor protein. We are grateful to Ronit Spotts and Yuan Ching Liu, of the K. S. Matthews laboratory, for providing much of the protein used in these studies, for carrying out the gel mobility shift assays, and for their advice in protein purification. Dr. Hans Liao of the Biotechnology Center of the University of Wisconsin—Madison graciously offered his assistance in transforming and growing the overproducing strain. Finally, we are indebted to Drs. K. S. Matthews, Jannette Carey, and Guy Page for careful reading of the manuscript and many helpful discussions.

## REFERENCES

Alcala, J. R., Cratton, E., & Jameson, D. M. (1985) *Anal. Instrum. (NY) 14*, 225–250.

Alcala, J. R., Gratton, E., & Prendergast, F. G. (1987) *Biophys. J. 51*, 597–604.

Arvidson, D. A., Bruce, C., & Gunsalus, R. P. (1986) *J. Biol. Chem. 261*, 238–243.

Baringa, M. (1991) *Science 251*, 1176–1177.

Bass, S., Sugiono, P., Arvidson, D. N., Gunsalus, R. P., & Youderian, P. (1987) *Genes Dev. 1*, 565–572.

Beechem, J. M., Gratton, E., Ameloot, M., Knutson, J. R., & Brand, L. (1989) in *Fluorescence Spectroscopy: Principles and Techniques* (Lakowicz, J. R., Ed.) Vol. I, Plenum Press, New York.
Benezra, R., Davis, R. L., Lockshon, D., Turner, D. L., & Weintraub, H. (1990) *Cell 61*, 49.
Bennett, G. N., Schweingruber, M. E., Brown, K. D., Squires, C., & Yanofsky, C. (1976) *Proc. Natl. Acad. Sci. U.S.A. 73*, 2351–2355.
Blackwood, E. M., & Eisenman, R. N. (1991) *Science 251*, 1211–1217.
Bowie, J. U., & Sauer, R. T. (1989) *Biochemistry 28*, 7139–7143.
Brown, K. D. (1969) *Genetics 60*, 31–48.
Carey, J. (1988) *Proc. Natl. Acad. Sci. U.S.A. 85*, 975–979.
Carey, J. (1989) *J. Biol. Chem. 264*, 1941–1945.
Carey, J. (1991) *Methods Enzymol.* (in press).
Chou, W.-Y., & Matthews, K. S. (1989) *J. Biol. Chem. 264*, 18314–18319.
Diamond, M. I., Miner, J. N., Yoshinaga, S. K., & Yamamoto, K. R. (1990) *Science 249*, 1266–1271.
Fernando, T. M. (1991) Ph.D. Dissertation, University of Illinois, Urbana, IL.
Gentz, R., Rauscher, F. J., III, Abate, C., & Curran, T. (1989) *Science 243*, 1695–1699.
Graddis, T. J., Klig, L. S., Yanofsky, C., & Oxender, D. L. (1988) *Proteins: Struct., Funct., Genet. 4*, 173–181.
Gratton, E., & Limkeman, M. (1983) *Biophys. J. 44*, 315–323.
Gratton, E., Limkeman, M., Lakowicz, J., Maliwal, B. P., Cherek, H., & Laczko, G. (1984) *Biophys. J. 46*, 479–486.
Guest, C. R., Hochstrasser, R. A., Dupuy, C. G., Allen, D. J., Benkovic, S. J., & Millar, D. P. (1991) *Biochemistry 30*, 8759–8770.
Gunsalus, R. P., & Yanofsky, C. (1980) *Proc. Natl. Acad. Sci. U.S.A. 77*, 7117–7121.
Gunsalus, R. P., Miguel, A. G., & Gunsalus, G. L. (1986) *J. Bacteriol. 167*, 272–278.
He, J.-J., & Matthews, K. S. (1989) *J. Biol. Chem. 265*, 731–737.
Hurlburt, B. K., & Yanofsky, C. (1990) *J. Biol. Chem. 265*, 7853–7858.
Jameson, D. M. (1978) Ph.D. Dissertation, University of Illinois, Urbana, IL.
Joachimiak, A., Kelley, R. L., Gunsalus, R. P., Yanofsky, C., & Sigler, P. B. (1983) *Proc. Natl. Acad. Sci. U.S.A. 80*, 668–672.
Kinosita, K., Kawato, S., & Ikegami, A. (1977) *Biophys. J. 20*, 289–305.
Klig, L. S., Crawford, I. P., & Yanofsky, C. (1987) *Nucleic Acids Res. 15*, 5339–5351.
Kouzerides, T., & Ziff, E. (1989) *Nature 340*, 568–570.
Kumamoto, A. A., Millar, W. G., & Gunsalus, R. P. (1987) *Genes Dev. 1*, 556–564.
Lambooy, P. K., Steiner, R. F., & Sternberg, H. (1982) *Arch. Biochem. Biophys. 217*, 17–528.
Lipari, G., & Szabo, A. (1980) *Biophys. J. 30*, 489–506.
Otwinowski, Z., Schevitz, R. W., Zhang, R.-G., Lawson, C. L., Joachimiak, A., Marmorstein, R. Q., Luisi, B. F., & Sigler, P. B. (1988) *Science 335*, 321–329.
Paluh, J. L., & Yanofsky, C. (1986) *Nucleic Acids Res. 14*, 7851–7860.
Perrin, F. (1926) *J. Phys. Radium 1*, 390–401.
Piston, D. W., Marriott, G., Radiveyovich, T., Clegg, R. M., Jovin, T. M., & Gratton, E. (1989) *Rev. Sci. Instrum. 60*, 2596–2600.
Prendergast, G. C., Lawe, D., & Ziff, E. B. (1991) *Cell 65*, 395–407.
Rose, J. K., & Yanofsky, C. (1974) *Proc. Natl. Acad. Sci. U.S.A. 71*, 3134–3138.
Rose, J. K., Squires, C. L., Yanofsky, C., Yang, H.-L., & Zubay, G. (1973) *Nature (London), New Biol. 245*, 133–137.
Royer, C. A., Rusch, R. M., & Scarlata, S. F. (1989) *Biochemistry 28*, 6631–6637.
Royer, C. A., Chakerian, A. E., & Matthews, K. S. (1990) *Biochemistry 29*, 4959–4966.
Schevitz, R. W., Otwinowski, Z., Joachimiak, A., Lawson, C. L., & Sigler, P. B. (1985) *Nature 317*, 782–786.
Senear, D. F., & Ackers, G. K. (1990) *Biochemistry 29*, 6568–6577.
Staake, D., Walter, B., Kisters-Woike, B., von Wilcken-Bergmann, B., & Muller-Hill, B. (1990) *EMBO J. 9*, 1963–1967.
Steiner, R. F. (1983) in *Excited States of Biopolymers* (Steiner, R., Ed.) Plenum Press, New York.
Tasayco, M. L., & Carey, J. (1992) *Science* (in press).
Turner, R., & Tijan, R. (1989) *Science 243*, 1689–1694.
Weber, G. (1966) in *Fluorescence and Phosphorescence Analysis* (Hercules, D. M., Ed.) Interscience, New York.
Weintraub, H., Davis, R., Tapscott, S., Thayer, M., Krause, M., Benezra, R., Blackwell, T. K., Turner, D., Rupp, R., Hollenberg, S., Zhuang, Y., & Lassar, A. (1991) *Science 251*, 761–766.
Zhang, R.-g., Joachimiak, A., Lawson, C. L., Schevitz, R. W., Otwinowski, Z., & Sigler, P. B. (1987) *Nature 327*, 591–597.